Pollen, biomarker and stable isotope evidence of late Quaternary environmental change at Lake McKenzie, southeast Queensland

Pia Atahan[a,b,*], Henk Heijnis[a], John Dodson[a], Kliti Grice[b], Pierre Le Métayer[b], Kathryn Taffs[c], Sarah Hembrow[c], Martijn Woltering[b], Atun Zawadzki[a]

[a] Institute for Environmental Research, Australian Nuclear Science and Technology Organisation, Sydney, Locked Bag 2001, Kirrawee DC, NSW 2232, Australia

[b] WA-Organic and Isotope Geochemistry Centre, Department of Chemistry, Curtin University, GPO Box U1987, Perth, WA 6845, Australia

[c] Southern Cross Geoscience and School of Environment, Science and Engineering, Southern Cross University, PO Box 157, Lismore NSW 2480, Australia

* Corresponding author: email address: pia.atahan@ansto.gov.au; telephone: +61 2 9717 7261

Abstract

Unravelling links between climate change and vegetation response during the Quaternary is important if the climate-environment interactions of modern systems are to be fully understood. Using a sediment core from Lake McKenzie, Fraser Island, we reconstruct changes in the lake ecosystem and surrounding vegetation over the last ca. 36.9 cal kyr. Evidence is drawn from multiple sources, including pollen, micro-charcoal, biomarker and stable isotope (C and N) analyses, and is used to gain a better understanding of the nature and timing of past ecological changes that have occurred at the site. The glacial period of the record, from ca. 36.9-18.3 cal kyr BP, is characterised

by an increased abundance of plants of the aquatic and littoral zone, indicating lower lake water levels. High abundance of biomarkers and microfossils of the colonial green alga *Botryococcus* occur at this time and include large variation in individual botryococcene $\delta^{13}C$ values. A slowing or ceasing of sediment accumulation occurs during the time period from ca. 18.3-14.0 cal kyr BP. By around 14.0 cal kyr BP fire activity in the area was reduced, as was abundance of littoral plants and terrestrial herbs, suggesting wetter conditions from that time. The Lake McKenzie pollen record conforms to existing records from Fraser Island by containing evidence of a period of reduced effective precipitation commencing in the mid-Holocene.

Key words

Quaternary, *Botryococcus*, pollen, palaeoecology, Fraser Island, southeast Queensland

Introduction

Lake sediment is an important source of information about late Quaternary climate and environmental change in southeast Queensland, Australia. The region has produced long and high quality records focused on microfossils (pollen, diatoms and charcoal) and geochemistry, and these have been used to reconstruct past changes in vegetation, human activity and aeolian sedimentation (Longmore 1997; Longmore and Heijnis 1999; Donders et al. 2006; McGowan et al. 2008; Barr et al. 2013; Moss et al. 2013). Much of what is known about Quaternary environments in the subtropical region of Australia has come from lake records on North Stradbroke Island and Fraser Island, and records from these islands have recently been included in continent-scale climate syntheses produced by the OZ-INTIMATE project (Petherick et al. 2013; Reeves et al. 2013). Despite this region's importance in understanding factors driving climate in subtropical Australia, in comparison

to temperate regions it has a low density of sediment-based proxy records extending into the last glacial.

This study focuses on reconstructing past environmental change at a lake site on Fraser Island, using microfossil, biomarker and stable isotope analysis techniques. This study builds on previous work at the site, using diatom and branched glycerol dialkyl glycerol tetraether (GDGT) distributions (Hembrow and Taffs 2012; Hembrow et al. 2014; Woltering et al. 2014), and aims to broaden understanding of past environmental conditions at the site. Some key benefits of including biomarker and compound specific isotope techniques in studies of Quaternary-aged sediment have for example been discussed by Bianchi and Canuel (2011), Eglinton and Eglinton (2008) and Sachs et al. (2007) and importantly include the attainment of otherwise unavailable information about past isotope reservoirs and presence of organisms not associated with hard fossil remains.

Site Description

Lake McKenzie is a clear water oligotrophic lake located in an elevated inland area of Fraser Island, about 7 km from the western coastline (25°26'51" S, 153°03'12" E; Fig. 1). The lake has an area of about 94 ha, an elevation of 85 m above sea level and lies amongst dunes that reach 150 m in elevation. The lake is positioned above the regional groundwater table, and its relatively impermeable base-layer (a B-horizon) restricts downwards percolation of water (Timms 1986; Longmore 1998). The lake has no inflow or outflow creeks and thus is highly responsive to changes in precipitation and evaporation. Concentrations of total phosphorus are low (2-5 $\mu g\ L^{-1}$), as is pH (4.8 – 5.8), and dominant types of phytoplankton are *Sphaerocystis*, *Oocystis* and *Peridinium* (Bowling 1988; Hadwen et al. 2003). Living *Botryococcus* has not been reported in this lake, although it is reported in other perched lakes on Fraser Island (Bowling 1988). The lake lies within a national park that has been largely protected from industrial and residential development.

71 The Fraser Island landmass is composed of Quaternary-aged sand dunes that were formed
72 progressively during periods of lower sea level (Lees 2006). The climate is subtropical. Rainfall
73 derives mostly from south-easterly trade winds and tropical cyclones from the north. Mean monthly
74 rainfall for January and July is respectively around 160 and 90 mm, and mean monthly temperatures
75 are between 20 and 32°C in January and 12 and 23°C in July (Australian Bureau of Meteorology
76 2013). Precipitation patterns on Fraser Island are strongly influenced by topography, rainfall is
77 substantially higher in elevated areas on dune slopes (Longmore 1998)

78 The sandy soils of Fraser Island support a diverse range of vegetation communities, including
79 heathlands, woodlands, tall eucalypt forest, and closed rainforest. Local water table depth, nutrient
80 availability, soil salinity and local burning regimes are important influences on the structure and
81 composition of vegetation communities on the island. Common vegetation communities are
82 *Eucalyptus signata* - *Banksia* wallum heathland; coastal woodland, sedgeland and swamp; tall
83 eucalypt forest with *Syncarpia hillii* and *Lophostemon confertus*; and tall closed forest with rainforest
84 and *E. pilularis* (Ryan 2012). Vegetation on slopes surrounding Lake McKenzie is composed of tall
85 forest with *E. racemosa*, *E pilularis*, *E. microcorys*, *E. resinifera* and *Syncarpia hillii*. Dominant plants
86 of the littoral zone are *Baumea* spp., *Juncus* spp. and *Lepironia articulata* (Ryan 2012).

87

88 **Methods**

89 Sampling and Dating

90 The methods by which the Lake McKenzie cores were sampled and dated has been previously
91 described by Hembrow et al. (2014) and Woltering et al. (2014). Two adjacent sediment cores were
92 extracted from the centre of the deepest basin of Lake McKenzie in 2010, in 8.3 m water depth. The
93 five centimetre diameter cores (LM1 and LM2) were extracted using a gravity corer, extruded on the
94 lake edge, and sliced into either 0.25 cm thick (LM1) or 1 cm thick (LM2) samples. Total un-extruded

core length was measured at five to ten centimetre intervals during sampling to monitor any loss of core recovery. Samples were placed in individual plastic zip-lock bags before being transported and stored in laboratory freezers.

The cores were composed of uniformly dark organic-rich mud, with no visible alterations in colour or texture. With the exception of one large wood fragment recovered from core LM1, terrestrial plant macrofossils, such as leaves or seeds, were not encountered in the cores. For this reason, and in order to target terrestrially-derived carbon, pollen residues were prepared for AMS ^{14}C dating. Preparation of pollen residues for AMS ^{14}C dating involved sieving to collect a 10-150 µm size fraction, separation by heavy liquid flotation (LST; SG = 1.8) and treatment with NaOH (10%), HCl (10%) and H_2SO_4 (98%). Pre-treatment of the wood fragment involved acid-alkali-acid treatment and all samples were graphitised according to standard procedure at the Australian Nuclear Science and Technology Organisation (ANSTO) (Hua et al., 2001). Radiocarbon dates were calibrated using the IntCal09 calibration curve (Reimer et al. 2009). Calibrated ages in the text are followed with a 'cal kyr BP' post-fix, single calibrated dates mentioned in the text refer to the median age in the 2σ calibrated age-range.

Abundance of atmosphere-derived ^{210}Pb ($^{210}Pb_{unsupported}$) in the upper sediment was used to estimate recent sediment accumulation rates at Lake McKenzie. The method, which has been described in detail by Appleby and Oldfield (1978), Appleby and Oldfield (1992) and Appleby (2001), uses down-core change in $^{210}Pb_{unsupported}$ activity to calculate an accumulation rate based on the ^{210}Pb half-life of 22.26 ±0.22 years. $^{210}Pb_{unsupported}$ was estimated by subtracting activity of supported ^{210}Pb ($^{210}Pb_{supported}$), which was measured indirectly from its grandparent radioisotope Radium-226 (^{226}Ra), from total ^{210}Pb ($^{210}Pb_{total}$) activity, which was measured indirectly from its progeny polonium-210 (^{210}Po). Both the CIC (constant initial concentration) and the CRS (constant rate of supply) models (Appleby and Oldfield 1978; Appleby 2001) were applied and calendar ages estimated.

$^{210}Pb_{supported}$ and $^{210}Pb_{total}$ were measured in the upper 8.5 cm of core LM1. Between 0.18 and 1.23 g of sediment was prepared by heating the samples in HNO_3 at 60°C. Once evaporated, small amounts of H_2O_2 (10%) were added with heating until the reaction subsided. The samples were evaporated again before refluxing in a mixture of HNO_3 and HCl (1:3; 50-60°C) for at least 4 hours. Samples were subsequently redissolved in HCl (6M) and centrifuged to separate the supernatant from the residue. The supernatant was collected and processed to remove excess iron by diethyl ether solvent extraction. ^{210}Po and ^{209}Po were isolated by auto-deposition onto silver discs using $NH_2OH.HCl$. ^{226}Ra and ^{133}Ba were isolated by co-precipitation and collected as colloidal micro-precipitates on 0.1 µm Millipore VV membrane filters. The recovery of the preparation method was assessed using radioactive tracers ^{133}Ba (~85 Bq) for ^{226}Ra recovery and ^{209}Po (~0.2 Bq) for ^{210}Po recovery, which were added at the start of the sample processing procedure. The auto-plated polonium on the silver discs and the radium micro-precipitates on membrane filters were analysed using ORTEC alpha spectrometers to determine ^{210}Po and ^{226}Ra activities. ^{133}Ba was analysed using a HPGE gamma spectrometer.

Microfossil analysis

Thirty-two samples from core LM2 were prepared for microfossil analysis. This preparation involved sieving using a 125 µm mesh, treatment with HCl (10%), KOH (10%), HF (40%), acetolysis and mounting in glycerol. A known quantity of *Lycopodium* marker grains was added to each sample to allow for quantification of microfossils. Microfossils were counted under an Olympus BX50 microscope at 600x magnification and pollen was counted until 300 grains of terrestrial plant types were observed. Pollen identification was assisted by online resources (Newcastle Pollen Collection 2002; Australasian Pollen and Spore Atlas 2013) and published literature (Pike 1956). Results are presented as percentages of the total terrestrial pollen sum. Pollen zones were assigned on the basis

of a stratigraphically constrained cluster analysis (CONISS) (Grimm 1987) performed using Tilia software (v. 1.7.16) (Grimm 1992).

Micro-charcoal particle and *Botryococcus* colony concentrations were estimated using the point count method (Clark 1982). Micro-charcoal particles were identified based on their black or transparent grey colour and jagged outline and only particles with an axis longer than 10 µm were counted.

Total organic carbon (TOC), total nitrogen (TN) and bulk organic $\delta^{13}C$ and $\delta^{15}N$ analysis

All samples from core LM2 were analysed on a Delta V Advantage Continuous Flow Isotope Ratio Mass Spectrometer-Flash 2000 HT Elemental Analyser for C%, N%, $\delta^{13}C$ and $\delta^{15}N$. Nitrogen measurements were conducted on oven dried (40 °C), homogenised sediment. Carbon measurements were conducted on the same aliquots after they had been treated with HCl (10%) to remove any carbonate material present in the sample. The reference materials used were: CO_2 - calibrated against IAEA CH6 with a consensus value of 10.449‰ Vienna Peedee Belemnite (VPDB) (Coplen et al. 2006); N_2 - calibrated against IAEA N-1 with a consensus value of δ^{15}NAIR = +0.4‰ (Bohlke and Coplen, 1995); working soil standard AILS SSA (ANSTO Isotope Laboratory Standard - Simulated Soil Aliquot); and acetanilide. The results are reported relative to VPDB for C and air for N.

Lipid analysis

Twelve samples from core LM2 were extracted using a Soxhlet apparatus and pre-extracted cellulose thimbles. Extractions were performed on 3-5 g of dried and ground sediment for 24 hours, with a solvent mixture of dichloromethane and methanol (9:1). Activated copper turnings were added to the collection flask to remove elemental sulphur. Extracts were separated into two aliquots,

166 evaporated to dryness and weighed. Aliquots of each sample were initially prepared for GC-MS
167 analysis using the separation procedure described below. A modified separation procedure was then
168 performed on remaining aliquots of 6 samples, prior to analysis by isotope ratio monitoring (irm)-
169 GC-MS.

170 Aliquots of extracts were initially separated using a small column (50 mm x 5 mm) filled with
171 activated silica gel pre-eluted with *n*-Hexane. Extracts were progressively eluted with 2 ml of
172 *n*-Hexane (the saturated hydrocarbon fraction), 3:7 DCM: *n*-Hexane (the aromatic hydrocarbon
173 fraction) and 1:1 DCM: *n*-Hexane (the polar fraction). Known volumes of squalane (Fluka 85629)
174 were added to the saturated hydrocarbon fractions to allow for estimation of compound
175 concentrations. A modified separation procedure was performed on samples prior to irm-GC-MS
176 analysis in order to improve compound separation. Extracts were added to the top of a large column
177 (20 cm x 1 cm) filled with activated silica gel and eluted progressively with *n*-Pentane (2 bed-loads;
178 'F1' fraction); 3:7 DCM: *n*-Pentane (2 bed-loads; 'F2' fraction); and 1:1 DCM: *n*-Pentane (2 bed-loads;
179 'F3' fraction). Fractions 'F1' and 'F2' were combined and reseparating using a small column (50 mm x
180 5 mm) and eluted with *n*-Hexane (1 bed-load; 'F1a' fraction); *n*-Hexane (2 bed-loads; 'F1b' fraction);
181 *n*-Hexane (2 bed-loads; 'F1c' fraction); and 1:1 DCM: Methanol (2 bed-loads; 'F2' fraction). Aliphatic
182 and aromatic fractions were analysed by GC-MS. In some cases individual fractions were combined
183 prior to measurement by irm-GC-MS, in order to completely capture compounds that eluted across
184 fractions.

185 GC-MS analysis used a Hewlett Packard (HP) 5973 mass selective detector interfaced to HP 6890
186 gas chromatograph, fitted with a DB-5MS column (60 m x 0.25 µm i.d.; J and W Scientific). The GC
187 oven was programmed to increase from 40 °C to 300 °C at 3 °C min^{-1} with an initial hold time of 1
188 minute and a final hold time of 30 min. Samples were dissolved in *n*-Hexane and injected on-column
189 using a HP 6890 auto-sampler. Helium was used as the carrier gas, at a linear velocity of 28 cm s^{-1}
190 and the injector operating at constant flow. Typically the MS was operating at an ionisation energy

of 70 *eV*, a source temperature of 180 °C, with an electron multiplier voltage of 1800 V and a mass range of 50 to 550 amu.

Compound specific carbon isotope ratios were measured on an HP 6890 GC equipped with a HP6890 autosampler and interfaced to an Isoprime Micromass isotope ratio monitoring mass spectrometer. GC conditions were identical to those for GC-MS analysis described above. Each sample was analysed at least twice and $\delta^{13}C$ values are reported relative to VPDB. Maximum deviation between separate analyses was less than or equal to 0.5‰ for all but 7 of the biomarker $\delta^{13}C$ values reported here. Standard mixes with compounds of known isotope values were run at least between every two samples in order to monitor the stability of the system.

Results

Age model

The age model for Lake McKenzie has been previously described by Woltering et al. (2014) and was based on a deposition model that was constructed using OxCal (version 4.1) (Bronk Ramsey 2008, 2009) (Fig. 2). The deposition model excluded three dates that appeared to be outlying (OZN680, OZN681 and OZO411). Two of those dates (OZN680 and OZN681) were obtained at the same depth on core LM1, and appear to mark a sedimentary disturbance which may be related to the presence of the wood fragment. The third date relates to an age reversal of 1970 ^{14}C years which occurs between dates at 20-21 and 23-24 cm depths. In the absence of an obvious reason to exclude either date from the deposition model, Oxcal overall Agreement Indexes and Oxcal Outlier Analyses were compared to determine which had a higher likelihood of being erroneous. A low overall Agreement Index was produced when OZN685 excluded in a P_Sequence deposition model (58.2%), compared to that produced when OZO411 was excluded (65.3%), and Outlier Analyses indicated a higher posterior probability of OZO411 being an outlier compared with OZN685. Thus OZO411 was deemed to be a more likely outlier, and was excluded from the deposition model.

The sediment cores lacked visible lithological changes, however a large age difference of ca. 4.3 kyr was observed between contiguous samples obtained from 25-26 and 26-27 cm depths (OZN686 and OZ0412). Despite any visible indication of a break in sediment accumulation, the radiocarbon dates suggest a slowing or ceasing of sediment accumulation in the time interval of ca. 18.3-14.0 cal kyr BP.

Geochemical analyses

Marked changes in TOC%, TOC/TN and bulk organic matter $\delta^{13}C$ and $\delta^{15}N$ occur with depth (Fig. 3) and are characterised by a down-core increase in TOC/TN and decrease in $\delta^{15}N$ values. Nine compounds were observed that have been identified as botryococcenes (Fig. 4; Supplementary Material). Their identification was based on comparisons with published mass spectra of botryococcene compounds and Kováts indexes (Huang et al. 1999; Gao et al. 2007; de Mesmay et al. 2008). Botryococcenes from Lake McKenzie were also compared with a sample containing a compound previously identified as 1, 6, 17, 21-octahydrobotryococcene by Huang et al. (1999). A good match in elution time and mass spectra was found between this sample and the compound described here as the **A2** botryococcene. With the exception of the **C0** botryococcene, all botryococcenes display higher concentrations in the lower samples, below 26 cm depth (Fig. 3). The **C0** botryococcene however, shows a distinct down-core trend: concentrations of this compound peak at 17 cm and are low below 26 cm. Botryococcene compounds were observed to have $\delta^{13}C$ values in the range of -31.7‰ to -22.5‰ (Table 3).

Long chain *n*-alkanes observed in the Lake McKenzie samples had a strong odd-over-even predominance (Fig. 4) and had average chain lengths (C25- C33) between 27.6 and 29.1. Chain length was observed to increase with depth. $\delta^{13}C$ values of odd C23-C33 *n*-alkanes ranged from -38.6‰ to -30.3‰ (Table 3). A C_{20} HBI was also observed in the samples and showed higher concentrations in the upper samples and had a maximum concentration at 10 cm depth (Fig. 3).

240

241 Microfossil analyses

242 The pollen diagram for Lake McKenzie is presented in Figure 5. A depth constrained cluster analysis
243 (CONISS) was performed using all pollen types in order to identify pollen zones (Grimm 1987);
244 characteristics of each pollen zone are described below.

245

246 *Pollen zone LM2-1: 46-34 cm depth, ca. 36.9-26.9 cal kyr BP*

247 Pollen zone LM2-1 is characterised by high proportions of terrestrial herb pollen (mean = 15.3%), of
248 which Poaceae pollen is of highest abundance (11.1%), and is followed by *Amperea* (1.6%) and
249 Asteraceae (Tubuliflorae) (1.3%). Percentages of aquatic/littoral pollen are moderately high through
250 most of this zone (9.6%), and are dominated by Cyperaceae and Restionaceae. Casuarinaceae pollen
251 dominates the arboreal taxa (42.5%) and of the Myrtaceae pollen identified to genus level,
252 *Eucalyptus* and *Melaleuca* dominate. Moderate concentrations of micro-charcoal occur (195.9 cm^2
253 g^{-1}). Concentrations of *Botryococcus* colonies are high (323.6 cm^2 g^{-1}) compared to the overlying
254 zones.

255

256 *Pollen zone LM2-2: 34-26 cm depth, ca. 26.9-18.3 cal kyr BP*

257 Pollen zone LM2-2 is characterised by high percentages of pollen from aquatic/littoral plants (17.3%)
258 and relatively high percentages of terrestrial herb pollen (14.5%). Highest percentages of *Typha*
259 pollen occur in this zone (5.3%) and a sharp peak in *Typha* occurs at 33 cm depth. Cyperaceae also
260 occurs in high abundance (8.5%). A gradual replacement of Casuarinaceae with Myrtaceae pollen
261 occurs up-core through this zone. Terrestrial herb pollen is dominated by Poaceae (9.9%) and to a
262 lesser degree Asteraceae (Tubuliflorae) (1.6%), Chenopodiaceae (1.3%) and *Amperea* (0.8%).

Concentrations of micro-charcoal are high in this zone (519.9 cm^2 g^{-1}), peaking at 27 cm depth. *Botryococcus* colonies remain abundant (291.9 cm^2 g^{-1}).

Hiatus: 26-25 cm depth, ca. 18.3-14.0 cal kyr BP

An age difference of ca. 4.3 kyr is observed between contiguous samples taken from 25-26 and 26-27 cm depth. Although no lithological change occurs at this depth, the AMS ^{14}C dates suggest a hiatus is present spanning the time period from ca. 18.3-14.0 cal kyr BP.

Pollen zone LM2-3: 25-18 cm depth, ca. 14.0-6.1 cal kyr BP

A large change in the microfossil assemblage marks the lower boundary of this pollen zone. At the commencement of this zone, pollen of aquatic/littoral taxa are markedly reduced compared with the underlying zone (3.1%), as is Poaceae pollen (2.1%) and concentrations of both micro-charcoal (90.7 cm^2 g^{-1}) and *Botryococcus* colonies (39.2 cm^2 g^{-1}). Casuarinaceae pollen dominates the arboreal pollen (45.7%), and of the myrtaceous pollen types, *Lophostemon* and *Callistemon* are increased compared with the underlying zone (respectively 2.3% and 4.7%), while *Acmena* is decreased (0.2%). Percentages of *Monotoca* are higher (7.8%), while percentages of Asteraceae (Tubuliflorae) and Chenopodiaceae pollen are lower (respectively 0.2% and 0.4%) than the underlying zone.

Pollen zone LM2-4: 18-10 cm depth, ca. 6.1-2.5 cal kyr BP

Pollen zone LM2-4 is characterised by having the highest percentages of Myrtaceous pollen (59.6%). Percentages of Moraceae (0.5%) and *Dodonaea* (1.2%) are slightly increased compared with the underlying zones. Percentages of Casuarinaceae pollen are low (19.2%) while Myrtaceae pollen is high (59.1%). Pollen from aquatic/littoral taxa is slightly more abundant in this zone (3.7%) and two

peaks in their abundance occur at 15 and 10 cm depth. Micro-charcoal and *Botryococcus* concentrations also show slight increases around 15 and 10 cm depth, but on the whole are low in this zone. Percentages of Poaceae pollen are increased slightly (2.9%), compared with the underlying zone.

Pollen zone LM2-5: 10-0 cm depth, ca. 2.5-0 cal kyr BP

The uppermost pollen zone is characterised by reduced percentages of aquatic/littoral pollen (1.8%) and high percentages of *Monotoca* (12.6%). Casuarinaceae pollen is more abundant compared with the underlying zone (29.0%), as is *Dodonaea* (2.8%) and *Eucalyptus* (15.3%). Concentrations of micro-charcoal and *Botryococcus* colonies are slightly increased compared with the underlying zone (respectively 92.1 and 59.0 $cm^2 g^{-1}$), and show a small increase around 4 cm depth. Pollen from *Pinus* increases markedly at 4 cm depth.

Discussion

Chronological assessment of the Lake McKenzie record

Obtaining reliable radiocarbon age estimates on organic remains from lake sediments can be problematic, as lake sediments are susceptible to producing dates that appear greater than the date of sediment deposition. Processes leading to erroneously old radiocarbon ages commonly arise when organic matter that is depleted in ^{14}C in relation to the contemporaneous atmosphere is incorporated into the sediments *via* dissolved forms of carbon, or *via* organic remains transported to the lake after a period of storage in the catchment (Bjorck and Wohlfarth 2001; Walker et al. 2007).

Terrestrial plant remains are preferentially selected for radiocarbon dating as those remains are unaffected by lake water reservoir effects, and when those remains are relatively fragile they are

309 unlikely to withstand sediment reworking and long term storage processes in the catchment. They
310 thus have a ^{14}C composition that is consistent with the atmosphere contemporaneous to sediment
311 deposition (Bjorck and Wohlfarth 2001; Walker et al. 2007). A lack of suitable terrestrial macrofossils
312 in the Lake McKenzie cores led to pollen residues being targeted for radiocarbon dating. Pollen is an
313 advantageous material as it is primarily of terrestrial origin, it often has a short transport time from
314 site of production, and is commonly abundant in lake sediments (Vandergoes and Prior 2003).
315 However, prepared pollen fractions typically contain some organic detritus of unknown sources, and
316 this potentially influences radiocarbon age estimates (Bjorck and Wohlfarth 2001). And as pollen
317 exines are robust, pollen can be stored for lengthy periods of time on catchment slopes prior to
318 being deposited in lake sediments and thus potentially incorporate a time lag into radiocarbon age
319 estimates. At Lake McKenzie, the proportion of pollen transported to the lake *via* surface runoff is
320 minimised by the lack of inflowing water channels. Additionally, the lake catchment has been
321 predominantly vegetated with forest or woodland, and thus major events of sediment input would
322 be largely restricted to periods following vegetation disturbance, after severe fire or storm, for
323 example. Therefore time lags associated with sediment storage prior to deposition are unlikely to be
324 a major influence on age estimates at Lake McKenzie.

325 The exact reason for the observed slow rate of sediment accumulation at Lake McKenzie is
326 difficult to determine. Physical and chemical characteristics of Lake McKenzie are distinctly different
327 to Lake Allom and Hidden Lake, where faster rates of sediment accumulation have been reported
328 (Longmore 1998; Donders et al. 2006). Comparable rates of sediment accumulation are reported at
329 Old Lake Coomboo Depression (Longmore and Heijnis 1999) and both Lake McKenzie and Old Lake
330 Coomboo Depression are similar in the sense that they have relatively flat lake bed topographies, as
331 opposed to Hidden Lake which has steeper slopes. While Lake McKenzie, Lake Allom and Hidden
332 Lake are all oligotrophic and acidic (pH 4.0-5.8), Lake McKenzie has markedly clearer water, and
333 lower Total Phosphorus (≤5 µg l^{-1}), Total Nitrogen (≤70 µg l^{-1}) and Chlorophyll-a (≤0.2 µg l^{-1}) content
334 (Bowling 1988; Longmore 1998; Hadwen et al. 2003). These parameters may be related to a low rate

of lake productivity or high rate of sediment diagenesis, and thus a slower sediment accumulation rate at Lake McKenzie. Bioturbation does not appear to have played a major role at the Lake McKenzie coring site over the last 130 years as a clear monotonic decrease in $^{210}Pb_{unsupported}$ is observed in the upper part of the record. High water content, and low bulk density (Hembrow et al. 2013) in the upper layers of the sediment may account in part for the observed increase in sediment accumulation rate above 7 cm depth.

Environmental conditions at Lake McKenzie from ca. 36.9-18.3 cal kyr BP

The combined evidence presented here indicates that during the glacial period Lake McKenzie was shallow or ephemeral, and had an expanded littoral zone compared to present. Plants of the littoral or shallow water zone were abundant between ca. 36.9 and 18.3 cal kyr BP, as indicated by the high proportions of Cyperaceae and Restionaceae pollen in the record. Poaceae abundance is high at this time, which reflects either expanded grassy openings in surrounding vegetation, or an expanded littoral zone. The presence of long-chain *n*-alkanes with an odd-over-even predominance and $\delta^{13}C$ values within the range of -35.7 to -31.5‰ indicates a major source from terrestrial C3 plants (Eglinton and Hamilton 1967; Rieley et al. 1991). As do the $\delta^{13}C$ values of bulk organic matter which range from -28.5 to -27.7 ‰ (Smith and Epstein 1971; Tieszen 1991). High TOC/TN values suggest emergent and terrestrial plants are a dominant source of organic matter to the lake sediment (Bianchi and Canuel 2011), however caution in the interpretation of TOC/TN ratios is required at Lake McKenzie as *Botryococcus braunii* is known to produce bulk organic matter with high values. TOC/TN ratios greater than 20 have previously been observed for the algal colonies (Grice et al. 1998, 2001; Huang et al. 1999).

The green colonial alga *Botryococcus braunii* is the likely source of the botryococcene compounds observed in the Lake McKenzie sediments (Maxwell et al. 1968; Metzger et al. 1991). Down-core

359 changes in abundance of botryococcenes and microfossils of *Botryococcus* show similar variation
360 (Fig. 3 and 5), with highest abundance of both proxies occurring in two separate periods, at around
361 36.0-30.8 cal kyr BP and 23.5-20.3 cal kyr BP. The reason for the high abundance of *Botryococcus*
362 during the glacial period is not known, but could be linked to factors such as the nutrient status of
363 the lake water, or the presence of other phytoplankton with faster growth rates at the site. These
364 factors influence the modern distribution of the algae (Cook et al. 2011). The lower atmospheric CO_2
365 partial pressure of the glacial period would presumably have been favourable to this green alga, as it
366 has a CO_2 concentrating mechanism (Street-Perrott et al. 1997; Huang et al. 1999). The modern
367 distribution of *Botryococcus* is broad and the alga appears to have a wide ranging environmental
368 tolerance, however the alga is most commonly observed in freshwater oligotrophic lakes and ponds
369 (Cook et al. 2011) and its presence has previously been used to understand past changes in
370 eutrophication resulting from human activity (Smittenberg et al. 2005).

371 Botryococcene $\delta^{13}C$ values for the glacial period of the record range from -31.7‰ to -22.5‰ and
372 this is within the range of botryococcenes observed in Quaternary lake sediments at other sites (e.g.
373 Grice et al. 1998; Huang et al. 1999; Smittenberg et al. 2005; Gao et al. 2007; Grossi et al. 2012). This
374 large range in $\delta^{13}C$ values is seen in a single sample from 27 cm depth (Table 3). Wide and
375 contemporaneous variation in $\delta^{13}C$ values of botryococcenes has previously been observed, and
376 suggested to derive from their synthesis during successional periods of an algal bloom, when lake
377 water characteristics such as dissolved nutrients, pH and dissolved CO_2 were undergoing alteration
378 (Huang et al. 1999). This is a potential cause for the wide range in $\delta^{13}C$ values observed within the
379 one centimetre thick samples from the Lake McKenzie core.

380 Although the number of $\delta^{13}C$ values obtained on individual botryococcene compounds from Lake
381 McKenzie is small, a $\delta^{13}C$ maximum occurs in zone LM2-2 (ca. 26.9 - 18.3 cal kyr BP) (Table 3), and
382 this ^{13}C enrichment is also observed in the C29, C31 and C33 *n*-alkanes from this zone. The timing of
383 this apparent carbon isotope excursion corresponds with the terminal period of the last glacial and a

384 similarly timed positive shift in botryococcene $\delta^{13}C$ values has previously been observed in a lake
385 record from Mt Kenya (Huang et al. 1999). While the magnitude of the shift is greater in the Mt
386 Kenya record, the proposed cause for the isotopic shift at that site, from the depletion of CO_2(aq)
387 under the lower atmospheric pCO_2 of the LGM, may also explain the observed shift to more positive
388 botryococcene $\delta^{13}C$ values at Lake McKenzie.

389 Cooler conditions at Lake McKenzie during the glacial are suggested by the slightly higher
390 abundance of Asteraceae (Tubuliflorae). Previous work on GDGT distributions at Lake McKenzie,
391 using a global soil calibration, estimated mean annual air temperature to have been 4.1 °C cooler at
392 the site around 18.8 cal. kyr BP compared to present (Woltering et al. 2014).

393 Micro-charcoal particles are abundant during the glacial period of the record and reflect a higher
394 frequency and/or intensity of burning, probably as a result of dryer conditions. The influence of
395 humans on fire activity at Lake McKenzie during the glacial period is difficult to discern however. The
396 record does not extend far enough into the past to capture the initial occupation of the Australian
397 continent, and the record does not contain information about short-term alterations in fire activity,
398 as the time resolution for each sample is low. The presence of humans in SEQ during the glacial
399 period is confirmed by the occupation of Wallen Wallen Creek site on North Stradbroke Island
400 around 21,800 ^{14}C yr BP (Neal and Stock 1986; Ulm 2011). However, very little is known about pre-
401 Holocene human occupation of this area, as an extremely low number of archaeological sites have
402 been discovered (Bowdler 2010). In a continent that was dryer, windier and cooler than present
403 (Harrison and Dodson 1993; Hesse et al. 2004; Williams et al. 2009), resources available on Fraser
404 Island - from perched lakes, swamps and rainforest refugia for example – would seemingly have
405 been attractive to people. However further archaeological work is required to understand the extent
406 of human-induced fire activity on Fraser Island and on the nearby mainland.

407

Deglaciation

The observed ceasing or slowing of sediment accumulation at Lake McKenzie during deglaciation (ca. 18.3-14.0 cal kyr BP) is likely to have been caused by the lake becoming perennially or intermittently dry. Perched lake sediments are prone to hiatuses, due to their sensitivity to change in precipitation and evaporation (Verschuren 2003). A hiatus is reported in the Lake Allom record, persisting to around 12.0 cal kyr BP (Donders et al. 2006), and while detection of hiatuses in the Old Lake Coomboo Depression (OLCD) record is restricted by the low frequency of radiocarbon dates, a sandy layer bounded by radiocarbon dates of ca. 26.0 and 14.5 cal kyr BP has been suggested to indicate dry conditions (Longmore and Heijnis 1999). Although the presence of hiatuses limits the amount of information that can be gained, all three of the lake sediment records that extend into the glacial that are now available from Fraser Island contain evidence of dry conditions occurring between the time period of ca. 18.3-14.5 cal kyr BP.

The timing of dry periods observed in Fraser Island records during deglaciation does not conform to climate shifts observed on North Stradbroke Island. There, vegetation reconstructions show arid periods occurring later than those on Fraser Island. The Native Companion Lagoon record shows evidence of dryer conditions at ca. 13.7 and 10.5 cal kyr BP; at Welsby Lagoon drying appears at ca. 14.0-12.0 cal. yr BP and 11.5 cal. kyr BP; and at Tortoise Lagoon drying appears at 14.0-12.0, 11.8 and 11.0 cal kyr BP (Moss et al. 2013). Higher resolution work in both regions, but particularly on or near Fraser Island, is required to more precisely understand the timing and synchroneity of deglaciation climate changes in southeast Queensland. However, as the islands are separated by more than 1.5 ° of latitude, a time lag in climate shifts occurring in the two areas is feasible given current understanding about changes that were occurring in offshore marine currents at that time. According to evidence from marine cores, the zone of separation of the East Australian Current (EAC) from the Australian continent gradually migrated southwards after the last glacial maximum, passing Fraser Island and then North Stradbroke Island (Bostock et al. 2006). This current is part of a

major circulation system transporting warm tropical waters southwards, and has the effect of warming ocean water east of Fraser and North Stradbroke Islands. Thus deglaciation change in the position of this current might have had a non-synchronous influence on precipitation regimes in southeast Queensland. However other factors, such as differences in the islands' topography or the effects of sea level rise, may also have affected local moisture regimes of the two regions.

Environmental conditions at Lake McKenzie since ca. 14.0 cal kyr BP

Deeper water conditions at the sampling site from around 14.0 cal kyr BP are suggested by the reduction in abundance of plants of the littoral and shallow water zones, and the reduced contribution of terrestrial or emergent plant organic matter in the lake sediments. Wetter conditions are also suggested by the denser vegetation at the site, indicated by the reduced abundance of Poaceae and Asteraceae, and reduced fire activity. *Monotoca* and *Lophostemon* are more abundant during the Holocene and may track the establishment of modern types of eucalypt forest at the site. Those taxa are abundant in the eucalypt forests that currently occur on the high dunes and sand plains of Fraser Island, including those surrounding Lake McKenzie (Ryan 2012).

Superimposed on the underlying trend of higher effective precipitation during the Holocene is evidence of a subtle reduction in moisture at the site, commencing around ca. 6.1 cal kyr BP and persisting to around 2.5 cal kyr BP, suggested by the small increase in littoral plants. This evidence for dryer conditions commencing around the mid-Holocene is consistent with previous findings from diatom remains at the site (Hembrow et al. 2013). However unlike the pollen record presented here, the diatom record showed shallower water conditions persisting to present. Other lake records on Fraser Island show evidence of dry conditions during the mid-Holocene. At Hidden Lake, a dry period is reported from ca. 9.5-2.6 cal kyr BP, and is further described as progressing from a period of falling groundwater levels from ca. 9.5-6.3 cal kyr BP, to stable and low groundwater levels from ca. 6.3-5.1

457 cal kyr BP, and to rising groundwater levels from ca. 5.1-2.6 cal kyr BP (dates are recalibrated using
458 the original ^{14}C dates reported by Longmore (1998)). At Lake Allom, dry conditions are the proposed
459 cause for a sedimentary hiatus spanning from ca. 6.5-5.4 cal kyr BP (Donders et al. 2006), afterwhich
460 a period of moist conditions and rising lake levels is reported, persisting to ca. 3.0 cal kyr BP. Large-
461 scale synthesis studies of palaeoclimate records conclude conditions across eastern Australia to have
462 been more variable or dryer from around 6-5 cal kyr BP, and suggest this to have been due to an
463 increasing intensity of the El Niño Southern Oscillation (ENSO) (Donders et al. 2007; Petherick et al.
464 2013; Reeves et al. 2013). As the area of influence of ENSO is wide, its influence on climates of
465 eastern Australia is expected to have been synchronous (Donders et al. 2007). The return to wetter
466 conditions in the late Holocene at some Fraser Island sites contrasts with the general trend for
467 eastern Australia, and suggests that local factors may have been an important influence on the
468 island's hydrological regimes during the late Holocene.

469 Unlike other botryococcenes detected in the Lake McKenzie record, the **C0** botryococcene has a
470 maximum concentration at ca. 5.5 cal kyr BP (Fig. 3). This unique down-core trend of the **C0**
471 botryococcene could be explained by: 1) more than one race of *B. braunii* occurring in the lake over
472 time; or 2) the same organism synthesising different compounds at different times during the lake's
473 history. Further work on the alga and its biomarkers is required to determine whether
474 environmental factors were driving the observed down-core changes in botryococcene distributions
475 at Lake McKenzie.

476 Despite the apparent increase in human occupation of southeast Queensland during the mid-
477 Holocene (Ulm and Hall 1996; Ulm 2011), evidence of human activity in the form of large shifts in
478 fire activity or vegetation composition are absent in the Lake McKenzie record. This contrasts with
479 lake records from parts of North Stradbroke Island where increased burning is detected from the
480 mid- to late-Holocene and is linked with intensified human activity (Moss et al. 2013). Despite the
481 absence of human impact evidence in Fraser Island sediment records, archaeological investigations

find occupation of the mainland adjacent to Fraser Island to date to at least ca. 5.5 cal kyr BP (McNiven 1992) and occupation of Fraser Island itself to date to ca. 3 cal kyr BP (Ulm 2011). This mismatch highlights the need for further palaeoecological and archaeological work to better understand past human activity in the region.

Conclusions

The Lake McKenzie record provides a reconstruction of changes to ecosystem composition occurring over the last ca. 36.9 cal kyr, inferred from sedimentary micro-fossils, biomarkers and stable isotope ratios (C and N). Elevated abundance of littoral plants at the site and increased contribution of allochthonous organic matter to the lake sediment, along with increased abundance of terrestrial herbs, is interpreted as reflecting sustained dry conditions to at least ca. 18.3 cal kyr BP. The underlying trend for increasing effective precipitation after ca. 14.0 cal kyr BP is interrupted ca. 6.1 cal kyr BP, when a subtle shift towards dryer conditions is detected in the pollen record. This conforms to other evidence of mid-Holocene aridity on the island, and in the broader eastern Australian region. Abundance of both fossil *Botryococcus* colonies and *Botryococcus*-derived biomarkers indicate that maximum growth of this colonial green alga occurred during the glacial period, when conditions were drier and cooler, and surrounding vegetation was sparser and more prone to burning. The evidence presented here for the Lake McKenzie sediment record contributes to the understanding of spatial and temporal variability of ecological changes occurring on Fraser Island and in subtropical eastern Australia, and permits a better assessment of the significance of those ecological shifts in a regional context.

Acknowledgements

Janelle Stevenson is thanked for preparing the pollen residues. Linda Barry and Kerry Wilsher are thanked for assistance associated with sampling. Jack Goralewski and Daniela Fierro are thanked for undertaking ^{210}Pb dating, and Fiona Bertuch and Alan Williams are thanked for assisting with AMS ^{14}C dating. Stephen Clayton and Geoff Chidlow are thanked for technical assistance associated with GCMS and GC-IRMS measurements. Rene Diocares is thanked for assistance with EA-IRMS measurements. We thank Lorenz Schwark for helpful discussions about the research project and Yongsong Huang for generously providing a sample for compound comparison.

Pierre Le Métayer and Kliti Grice were supported by an ARC Discovery grant awarded to Kliti Grice. The Australian Nuclear Science and Technology Organisation (ANSTO) and The Institute for Geoscience Research at Curtin University provided funding for this project.

Formatted: Line spacing: Double

516 **References**

517 Appleby PG, Oldfield F (1978) The calculation of lead-210 dates assuming a constant rate of supply of
518 unsupported ^{210}Pb to the sediment. Catena 5: 1-8

519 Appleby PG, Oldfield F (1992) Application of ^{210}Pb to sediment studies. In: Ivonavich M, Harmon RS
520 (eds) Uranium-series disequilibrium: applications to earth, marine and environmental science.
521 Oxford University Press, Oxford, pp 731-778

522 Appleby PG (2001) Chronostratigraphic techniques in recent sediments. In: Last WM, Smol JP (eds)
523 Tracking environmental change using lake sediments, Volume 1: Basin analysis, coring and
524 chronological techniques. Kluwer Academic Publishers, Dordrecht, pp 171-203

525 Australasian Pollen and Spore Atlas (2013) Australasian Pollen and Spore Atlas. Canberra, ACT,
526 Australia. http://apsa.anu.edu.au/

527 Australian Bureau of Meteorology (2013) Australian Government. http://www.bom.gov.au/

528 Barr C, Tibby J, Marshall JC, McGregor GB, Moss PT, Halverson GP, Fluin J (2013) Combining
529 monitoring, models and palaeolimnology to assess ecosystem response to environmental
530 change at monthly to millennial timescales: the stability of Blue Lake, North Stradbroke Island,
531 Australia. Freshwater Biol 58: 1614-1630

532 Bianchi TS, Canuel EA (2011) Chemical biomarkers in aquatic ecosystems. Princeton University Press,
533 Princeton, New Jersey

534 Bjorck S, Wohlfarth B (2001) ^{14}C chronostratigraphic techniques in paleolimnology. In: Last WM,
535 Smol JP (eds) Tracking environmental change using lake sediments. Volume 1: Basin analysis,
536 coring and chronological techniques. Kluwer Academic Publishers, Dordrecht, pp 205-245

537 Bohlke JK, Coplen TB (1995) Interlaboratory comparison of reference materials for nitrogen isotope
538 ratio measurements, taken from an IAEA technical report, References and intercomparison
539 materials for stable isotopes of light elements. IAEA-TECHDOC-825, September 1995

540 Bostock HC, Opdyke BN, Gagan MK, Kiss AE, Fifield LK (2006) Glacial/interglacial changes in the East
541 Australian current. Clim Dynam 26, 645-659

542 Bowdler S (2010) The empty coast: conditions for human occupation in southeast Australia during
543 the late Pleistocene. In: Haberle S, Stevenson J, Prebble M (eds) Altered ecologies: fire climate
544 and human influence. Terra Australis 32. ANU EPress, Canberra, pp 178-186

545 Bowling LC (1988) Optical properties, nutrients and phytoplankton of freshwater coastal dune lakes
546 in south-east Queensland. Aust J Freshw Res 39: 805-815

547 Bronk Ramsey C (2008) Deposition models for chronological records. Quat Sci Rev 27: 42-60

548 Bronk Ramsey C (2009) Bayesian analysis of radiocarbon dates. Radiocarbon 51: 337-360

549 Clark RL (1982) Point count estimation of charcoal in pollen preparations and thin sections of
550 sediment. Pollen et Spores 24: 523-535

551 Cook EJ, Van Geel B, Van der Kaars S, van Arkel J (2011) A review of the use of non-pollen
552 palynomorphs in palaeoecology with examples from Australia. Palynology 35: 155-178

553 Coplen TB, Brand WA, Gehre,M, Gröning M, Meijer HAJ, Toman B, Verkouteren RM (2006) After two
554 decades a second anchor for the VPDB $\delta^{13}C$ scale. Rapid Commun Mass Spectrom 20: 3165-
555 3166

556 de Mesmay R, Metzger P, Grossi V, Derenne S (2008) Mono- and dicyclic unsaturated triterpenoid
557 hydrocarbons in sediments from Lake Masoko (Tanzania) widely extend the botryococcene
558 family. Org Geochem 39: 879-893

559 Donders TH, Wagner F, Visscher H (2006) Late Pleistocene and Holocene subtropical vegetation
560 dynamics recorded in perched lake deposits on Fraser Island, Queensland, Australia.
561 Palaeogeogr, Palaeoclim, Palaeoecol 241: 417-439

562 Donders TH, Haberle SG, Hope G, Wagner F, Visscher H (2007) Pollen evidence for the transition of
563 the Eastern Australian climate system from the post-glacial to the present-day ENSO mode.
564 Quat Sci Rev 26: 1621-1637

565 Eglinton G, Hamilton RJ (1967) Leaf epicuticular waxes. Science 156: 1322-1335

566 Eglinton TI, Eglinton G (2008) Molecular proxies for paleoclimatology. Earth Planet Sci Lett 275: 1-16

567 Gao M, Simoneit BRT, Gantar M, Jaffé R (2007) Occurrence and distribution of novel botryococcene
568 hydrocarbons in freshwater wetlands of the Florida Everglades. Chemosphere 70: 224-236

569 Grice K, Schouten S, Nissenbaum A, Charrach J, Sinninghe Damsté JS (1998) A remarkable paradox:
570 sulfurised freshwater algal (*Botryococcus braunii*) lipids in an ancient hypersaline euxinic
571 ecosystem. Org Geochem 28: 195-216

572 Grice K, Audino M, Boreham CJ, Alexander R, Kagi RI (2001) Distribution and stable carbon isotopic
573 compositions of biomarkers in torbanites from different palaeogeographical locations. Org
574 Geochem 32: 1195-1210

575 Grimm EC (1987) Coniss: a fortran 77 program for stratigraphically constrained cluster analysis by
576 the method of incremental sum of squares. Comput and Geosci 13: 13-35

577 Grimm EC (1992) Tilia and Tilia-graph: pollen spreadsheet and graphics programs. Program and
578 Abstracts, 8th International Palynological Congress, Aix-en-Provence [France]

579 Grossi V, de Mesmay R, Bardoux G, Metzger P, Williamson D, Derenne S (2012) Contrasting
580 variations in the structure and stable carbon isotopic composition of botryococcenes through
581 the last glacial-interglacial transition in Lake Masoko (southern Tanzania). Org Geochem 43:
582 150-155

583 Hadwen WL, Arthington AH, Mosisch TD (2003) The impact of tourism on dune lakes on Fraser
584 Island, Australia. Lakes Reserv: Res and Manag 8: 15-26

585 Harrison S, Dodson JR (1993) Climates of Australia and New Guinea since 18,000 yrs BP. In: Wright Jr
586 HE, Kutzbach JE, Webb III T, Ruddiman WF, Street-Perrott FA, Bartlein PJ (eds) Global climates
587 since the last glacial maximum. University of Minnesota Press, Minnesota, pp 265-293

588 Hembrow S, Taffs KH (2012) Water quality changes in Lake McKenzie, Fraser Island, Australia: a
589 Palaeolimnological approach. Aust Geogr 43: 291-302

590 Hembrow S, Taffs K, Atahan P, Parr J, Zawadzki A, Heijnis H (2014) Diatom community response to
591 climate variability over the past 37,000 years in the sub-tropics of the Southern Hemisphere.
592 Sci Total Environ 468-469: 774-784

593 Hesse PP, Magee JW, van der Kaars S (2004) Late Quaternary climates of the Australian arid zone: a
594 review. Quat Int 118-119: 87-102

595 Hua Q, Jacobsen GE, Zoppi U, Lawson EM, Williams AA, Smith AM, McGann MJ (2001) Progress in
596 radiocarbon target preparation at the Antares AMS centre. Radiocarbon 43: 275-282.

597 Huang Y, Street-Perrott FA, Perrott RA, Metzger P, Eglinton G (1999) Glacial-interglacial
598 environmental changes inferred from molecular and compound-specific $\delta^{13}C$ analyses of
599 sediments from Sacred Lake, Mt. Kenya. Geochim Cosmochim Acta 63: 1383-1404

600 Lees B (2006) Timing and formation of coastal dunes in northern and eastern Australia. J Coast Res
601 22: 78-89

602 Longmore ME (1997) Quaternary Palynological Records from Perched Lake Sediments, Fraser Island,
603 Queensland, Australia: Rainforest, Forest History and Climatic Control. Aust J Bot 45: 507-526

604 Longmore ME (1998) The middle Holocene 'dry' anomaly on the mid-eastern coast of Australia:
605 calibration of paleowater depth as a surrogate for effective precipitation using sedimentary
606 loss on ignition in the perched lake sediments of Fraser Island. Palaeoclimates 3: 135-160

607 Longmore ME, Heijnis H (1999) Aridity in Australia: Pleistocene records of Palaeohydrological and
608 Palaeoecological change from the perched lake sediments of Fraser Island, Queensland,
609 Australia. Quat Int 57-58: 35-47

610 Maxwell JR, Douglas AG, Eglinton G, McCormick A (1968) The botryococcenes – hydrocarbons of
611 nove structure from the alga *Botryococcus braunii* Kützing. Phytochemistry 7: 2157-2171

612 McGowan HA, Petherick LM, Kamber BS (2008) Aeolian sedimentation and climate variability during
613 the late Quaternary in southeast Queensland, Australia. Palaeogeogr, Palaeoclim, Palaeoecol
614 265: 171-181

615 McNiven I (1992) Sandblow sites in the Great Sandy Region, coastal southeast Queensland:
616 implications for models of late Holocene rainforest exploitation and settlement restructuring.
617 Qld Archaeol Res 9: 1-16

618 Metzger P, Largeau C, Casadevall E (1991) Lipids and mcaromolecular lipids of the hydrocarbon-rich
619 microalga *Botryococcus braunii*. Progress in the chemistry of organic natural products 57: 1-
620 70

621 Moss PT, Tibby J, Petherick L, McGowan H, Barr C (2013) Late Quaternary vegetation history of North
622 Stradbroke Island, Queensland, eastern Australia. Quat Sci Rev 74: 257-272

623 Neal R, Stock E (1986) Pleistocene ocupation in the south-east Queensland coastal region. Nature
624 323: 618-621

625 Newcastle Pollen Collection (2002) Newcastle Pollen Collection, Newcastle, NSW, Australia.
626 http://www.geo.arizona.edu/palynology/nsw/index.html

627 Petherick L, Bostock H, Cohen TJ, Fitzsimmons K, Tibby J, Fletcher MS, Moss P, Reeves J, Mooney S,
628 Barrows T, Kemp J, Jansen J, Nanson G, Dosseto A (2013) Climatic records over the past 30 ka
629 from temperate Australia – a synthesis from the OZ-INTIMATE workgroup. Quat Sci Rev 74:
630 58-77

631 Pike KM (1956) Pollen morphology of Myrtaceae from the south-west Pacific area. Aust J Bot 4: 13-
632 53

633 Queensland Herbarium (2013) Regional Ecosystem Description Database (REDD). Version 6.1
634 (February 2013). Queensland Department of Science, Information Technology, Innovation and
635 the Arts: Brisbane

636 Reeves JM, Barrows TT, Cohen TJ, Kiem AS, Bostock HC, Fitzsimmons KE, Jansen JD, Kemp J, Krause
637 C, Petherick L, Phipps SJ (2013) Climate variability over the last 35,000 years recorded in
638 marine and terrestrial archives in the Australian region: an OZ-INTIMATE compilation. Quat Sci
639 Rev 74: 21-34

640 Reimer PJ, Baillie MGL, Bard E, Bayliss A, Beck JW, Blackwell PG, Bronk Ramsey C, Buck CE, Burr GS,
641 Edwards RL, Friedrich M, Grootes PM, Guilderson TP, Hajdas I, Heaton TJ, Hogg AG, Hughen
642 KA, Kaiser KF, Kromer B, McCormac FG, Manning SW, Reimer RW, Richards DA, Southon JR,
643 Talamo S, Turney CSM, van der Plicht J, Weyhenmeyer CE (2009) INTCAL09 and Marine 09
644 radiocarbon age calibration curves, 0-50,000 years cal BP. Radiocarbon 51: 1111-1150

645 Rieley G, Collier RJ, Jones DM, Eglinton G, Eakin PA, Fallick AE (1991) Sources of sedimentary lipids
646 deduced from stable carbon-isotope analyses of individual compounds. Nature 352: 425-427

647 Ryan TS (2012) Technical Descriptions of Regional Ecosystems of Southeast Queensland. Queensland
648 Herbarium, Brisbane.

649 Sachs JP, Pahnke K, Smittenberg R, Zhang Z (2007) Biomarker indicators of past climate. In Elias S
650 (ed) Encyclopedia of Quaternary Science. Elsevier, Amsterdam, pp 19-48

651 Smith BN, Epstein S (1971) Two categories of $^{13}C/^{12}C$ ratios for higher plants. Plant Physiol 47: 380-
652 384

653 Smittenberg RH, Baas M, Schouten S, Sinninghe Damsté JS (2005) The demise of the alga
654 Botryococcus braunii from a Norwegian Fjord was due to early eutrophication. The Holocene
655 15: 133-140

656 Street-Perrott FA, Huang Y, Perrott RA, Eglinton G, Barker P, Khelifa LB, Harkness DD, Olago DO
657 (1997) Impact of lower atmospheric carbon dioxide on tropical mountain ecosystems. Science
658 278: 1422-1426

659 Tieszen LL (1991) Natural variations in the carbon isotope values of plants: implications for
660 archaeology, ecology, and palaeoecology. J Archaeol Sci 18: 227-248

661 Timms BV (1986) The coastal dune lakes of eastern Australia. In: De Deckker P, Williams WD (eds)
662 Limnology in Australia. Springer Nederlands, pp 421-432

663 Ulm S, Hall J (1996) Radiocarbon and cultural chronologies in southeast Queensland prehistory.
664 Tempus 6: 45-62

665 Ulm S (2011) Coastal foragers on southern shores: marine resource use in northeast Australia since
666 the late Pleistocene. In: Bicho NF, Haws JA, Davis LG (eds) Trekking the shore: changing
667 coastlines and the antiquity of coastal settlement. Springer, New York, pp 441-461

668 Vandergoes, M.J., Prior, C.A., 2003. AMS dating of pollen concentrates - a methodological study of
669 late Quaternary sediments from south westland, New Zealand. Radiocarbon 45, 479-491.

670 Verschuren D (2003) Lake-based climate reconstruction in Africa: progress and challenges.
671 Hydrobiologia 500: 315-330

672 Walker WG, Davidson GR, Lange T, Wren D (2007) Accurate lacustrine and wetland sediment
673 accumulation rates determined from ^{14}C activity of bulk sediment fractions. Radiocarbon 49:
674 983-992.

675 Williams M, Cook E, van der Kaars S, Barrows T, Shulmeister J, Kershaw P (2009) Glacial and deglacial
676 climatic patterns in Australia and surrounding regions from 35,000 to 10,000 years ago
677 reconstructed from terrestrial and near-shore proxy data. Quat Sci Rev 28: 2398-2419

678 Woltering M, Atahan P, Grice K, Heijnis H, Taffs K, Dodson J (2014) Glacial and Holocene terrestrial
679 temperature variability in subtropical east Australia: branched GDGT distributions in a
680 sediment core from Lake McKenzie. Quat Res 82: 132-145

681

682 **Table 1** Total ^{210}Pb, Supported ^{210}Pb, Unsupported ^{210}Pb, and particle size results for samples taken
683 from core LM1. Calendar age estimates using the CIC and CRS models are shown (Appleby and
684 Oldfield, 1978; Appleby, 2001). Both the original depths measured on core LM1 and the
685 corresponding depths on core LM2, as estimated using tie-points on Total Organic Carbon (%)
686 curves, are shown.

ANSTO ID	Depth Interval measured on core LM1 (cm)	Corresponding depth interval on core LM2 (cm)	Total ^{210}Pb (Bq kg^{-1})	Supported ^{210}Pb (Bq kg^{-1})	Unsupported ^{210}Pb* (Bq kg^{-1})	Particle size ≤62.5 µm (%)	Calculated CIC age (years)	Calculated CRS age (years)
M897	0.00-0.25	0.0-0.7	614 ± 12	14 ± 2	601 ± 12	74.0	5 ± 5	5 ± 2
M898	0.25-0.50	0.7-1.4	491 ± 24	18 ± 2	484 ± 24	74.0	15 ± 5	13 ± 4
M899	1.50-1.75	4.1-4.8	168 ± 6	19 ± 2	150 ± 6	90.0	65 ± 7	64 ± 8
M900	1.75-2.00	4.8-5.5	98 ± 4	15 ± 2	85 ± 5	77.6	75 ± 8	76 ± 9
M901	3.00-3.50	7.0-7.8	31 ± 1	20 ± 2	12 ± 2	83.9	131 ± 14	130 ± 11
M902	4.50-4.75	9.4-9.8	38 ± 1	27 ± 3	11 ± 3	78.9	-	-
M903	4.75-5.00	9.8-10.2	76 ± 4	63 ± 6	13 ± 7	79.9	-	-
N369	6.00-6.25	11.7-12.2	86 ± 4	22 ± 3	67 ± 5	69.9	-	-
N370	6.25-6.50	12.2-12.6	102 ± 5	42 ± 4	62 ± 6	72.5	-	-
N371	7.00-7.25	13.4-13.8	34 ± 2	33 ± 3	1 ± 4	73.3	-	-
N372	7.25-7.50	13.8-14.2	31 ± 2	33 ± 3	not detected	83.5	-	-
N373	8.00-8.25	15.0-15.2	63 ± 3	28 ± 3	36 ± 4	81.5	-	-
N374	8.25-8.50	15.2-15.5	63 ± 3	32 ± 3	32 ± 5	68.7	-	-

687 *decay corrected to a fixed date

688
689
690
691 **Table 2** AMS ^{14}C dates and calibrated age ranges for pollen residues and wood samples with depths
692 measured on core LM2.
693

Lab code	Depth (cm)	Core	Composition	^{14}C age (yrs BP)	Error (1σ)	Calibrated age-range (cal yr BP; 2σ)
OZN683	10-11	LM2	Pollen	2,395	± 35	2,183 - 2,654
OZN684	15-16	LM2	Pollen	3,785	± 35	3,931 - 4,230
OZN685	20-21	LM2	Pollen	6,485	± 50	7,260 - 7,431
OZO411	23-24	LM2	Pollen	4,515	± 40	5,044 - 5,309
OZN686	25-26	LM2	Pollen	12,110	± 70	13,786 - 14,148
OZO412	26-27	LM2	Pollen	15,100	± 70	18,026 - 18,589
OZN687	30-31	LM2	Pollen	18,670	± 100	21,872 - 22,545
OZN688	35-36	LM2	Pollen	23,270	± 120	27,785 - 28,499
OZN689	40-41	LM2	Pollen	30,940	± 190	34,924 - 36,280
OZN690	45-46	LM2	Pollen	31,870	± 180	35,575 - 36,783
OZN680	21.3-21.5	LM1	Pollen	19,150	± 210	22,330 - 23,428
OZN681	21.3-21.5	LM1	Wood	11,470	± 60	13,188 - 13,457

694

695

696

697 **Table 3** $\delta^{13}C$ values of *n*-alkanes and botryococcene compounds at different depths in core LM2. The
698 maximum per mil deviation of the measurements is shown in brackets below each $\delta^{13}C$ value. The
699 dash symbol indicates where no data is available.
700

	***n*-alkane $\delta^{13}C$ (‰)**						**Botryococcenes $\delta^{13}C$ (‰)**							
Depth (cm)	**C23**	**C25**	**C27**	**C29**	**C31**	**C33**	**A2**	**C1**	**C2**	**B3**	**B4**	**C3**	**C4**	**Zone**
1-2	-38.6 (0.0)	-36.6 (0.0)	-34.4 (0.4)	-33.0 (0.0)	-33.2 (0.2)	-33.0 (0.0)	-	-	-	-	-	-	-	LM2-5
10-11	-	-	-	-34.1 (0.1)	-33.5 (0.1)	-33.0 (0.0)	-	-	-	-	-	-	-	LM2-4
21-22	-35.4 (0.3)	-34.6 (0.1)	-32.7 (0.4)	-32.2 (0.0)	-32.7 (0.3)	-34.5 (0.0)	-	-	-25.7 (0.4)	-	-	-	-	LM2-3
24-25	-	-35.9 (0.0)	-32.4 (0.4)	-31.3 (1.5)	-31.9 (0.5)	-32.2 (0.3)	-	-24.6 (0.2)	-22.6 (0.2)	-	-	-24.1 (1.2)	-	
27-28	-	-35.7 (0.0)	-34.0 (1.5)	-31.5 (1.0)	-	-31.8 (0.2)	-32.0 (1.3)	-23.9 (0.2)	-22.5 (0.7)	-23.1 (0.5)	-24.0 (0.4)	-23.1 (0.2)	-24.5 (0.5)	LM2-2
31-32	-	-35.2 (0.2)	-34.3 (0.1)	-30.3 (0.0)	-31.9 (0.0)	-31.2 (0.2)	-29.8 (0.0)	-23.6 (0.2)	-24.3 (0.2)	-	-23.7 (0.1)	-22.8 (0.2)	-24.6 (0.1)	
38-39	-	-	-32.0 (0.7)	-32.7 (0.2)	-32.4 (0.0)	-31.9 (0.1)	-	-26.9 (0.1)	-23.6 (0.0)	-25.1 (0.2)	-26.2 (0.1)	-25.3 (0.2)	-27.2 (0.1)	LM2-1

701

702

703

Figure captions

Fig. 1 **A** location of the South Eastern Bioregion on the east coast of the Australian continent (red coloured area). **B** Vegetation map of Fraser Island (Queensland Herbarium, 2013). The white triangles mark locations of (1) Lake McKenzie; (2) Hidden Lake; (3) Old Lake Coomboo Depression (OLCD); and (4) Allom Lake.

Fig. 2 Age-depth diagram for Lake McKenzie incorporating AMS ^{14}C and ^{210}Pb ages. The IntCal09 calibration curve (Reimer et al., 2009) and the OxCal P_Sequence program (k = 4) (Bronk Ramsey, 2008, 2009) were used to construct the deposition model.

Fig. 3 Diagram showing elemental composition and stable isotope carbon and nitrogen isotope ratios measured for the Lake McKenzie core LM2. Concentrations of biomarker compounds are also shown as a sum of the 9 botryococcene compounds observed in the samples, individual concentrations of two botryococcenes (**A2** and **C0**) and concentrations of the C_{20} HBI. The shaded area indicates the location of the hiatus suggested by radiocarbon ages on contiguous samples.

Fig. 4 Total ion chromatogram of saturate fraction of Lake McKenzie core LM3, from **A**: 1 cm depth and **B**: 31 cm depth. Filled squares refer to *n*-alkanes and the number above the square refers to their carbon number. Compounds **A2**, **C1**, **C2**, **B3**, **B4**, **C3**, **C4** and **C5** are observed botryococcene compounds.

Fig. 5 Pollen diagram for Lake McKenzie core LM2. Pollen data is presented as percentages of the total terrestrial pollen sum; the units for total pollen are grains g^{-1}; and the units for micro-charcoal and *Botryococcus* are $cm^2\ g^{-1}$.

Supplementary Material

The Kováts indexes and diagnostic MS ions for botryococcene compounds identified in the Lake McKenzie sediments.

MF	MW	Compound	K.I.	Diagnostic ions in mass spectra (m/z)
$C_{34}H_{66}$	474	A2	2765	474 (9), 291 (22), 207 (7), 137 (44), 123 (50), 109 (61), 81 (100)
$C_{34}H_{62}$	470	C1	2775	470 (4), 455 (10), 231 (34), 203 (68), 177 (85), 109 (84), 81 (100)
$C_{34}H_{58}$	466	C0	2788	466 (3), 285 (7), 231 (11), 177 (100), 149 (40), 123 (79), 95 (78)
$C_{34}H_{64}$	472	C2	2800	472 (22), 443 (14), 233 (14), 178 (100), 123 (89), 109 (84), 83 (78)
$C_{34}H_{60}$	468	B3	2812	468 (10), 453 (4), 287 (27), 205 (12), 178 (43), 123 (100), 95 (77)
$C_{34}H_{64}$	472	B4	2823	472 (17), 443 (14), 233 (17), 178 (96), 164 (40), 83 (100), 57 (98)
$C_{36}H_{66}$	498	C3	2924	498 (14), 469 (6), 233 (8), 178 (78), 123 (84), 109 (84), 83 (100)
$C_{36}H_{68}$	500	C4	2967	500 (14), 471 (9), 233 (11), 178 (100), 123 (91), 109 (84), 57 (100)
$C_{37}H_{68}$	512	C5	3026	512 (14), 483 (5), 233 (8), 178 (81), 123 (81), 109 (77), 83 (100)

MF = molecular formula; MW = molecular weight; KI = pseudo Kováts retention index: $100_n + 100*[(R_x - R_n)/(R_{n+1} - R_n)]$ where x = compound of interest, *n* = carbon number of the nearest *n*-alkane eluting in front of x on the GC; *R* = retention time. The numbers in brackets following the diagnostic ions are the relative intensity compared to that of the base peak.

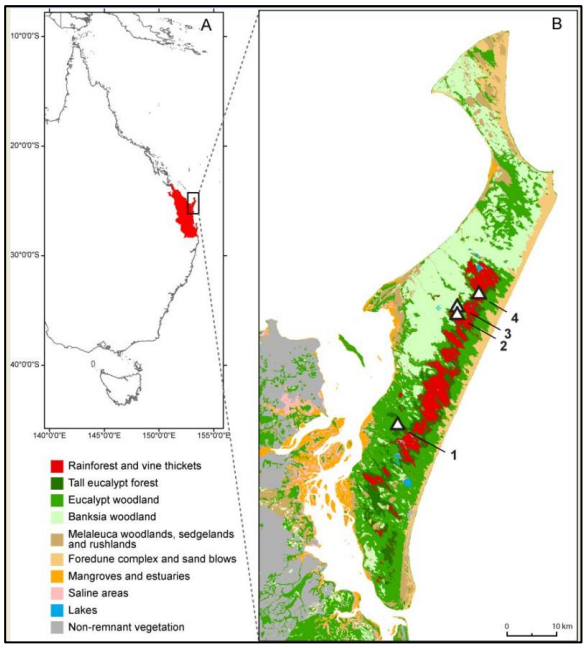

Figure 1

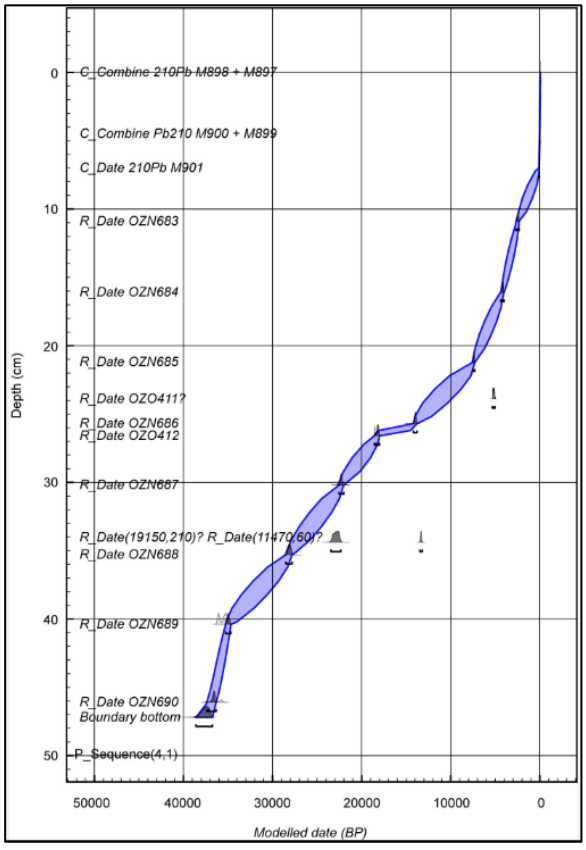

Figure 2

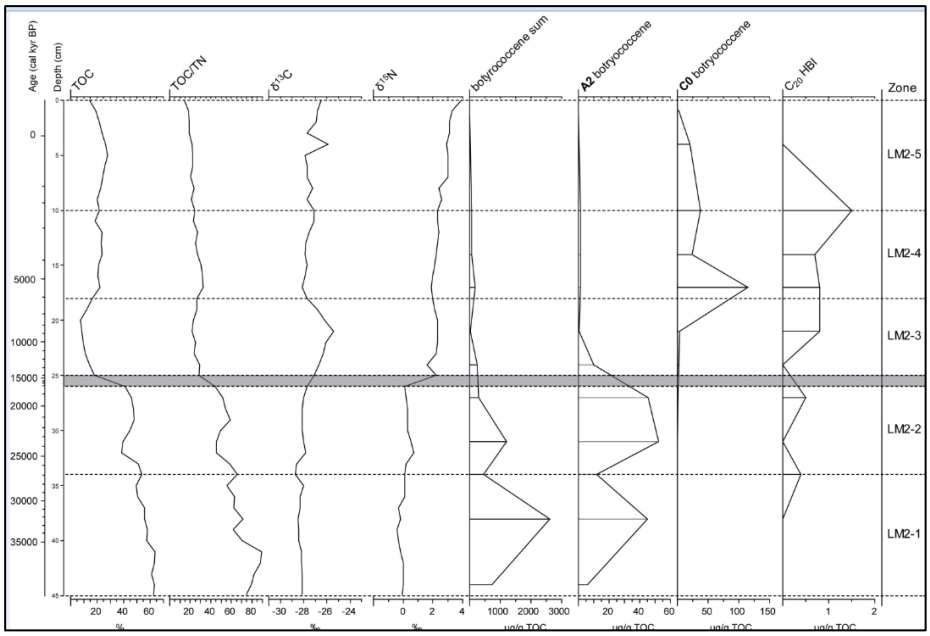

Figure 3

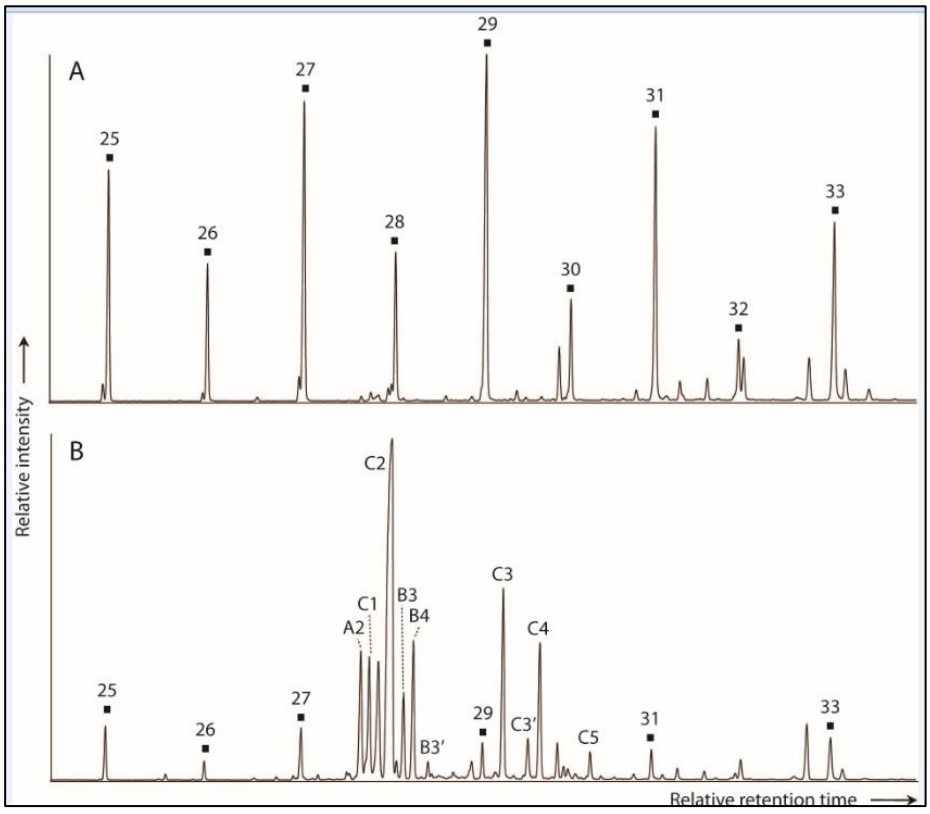

Figure 4

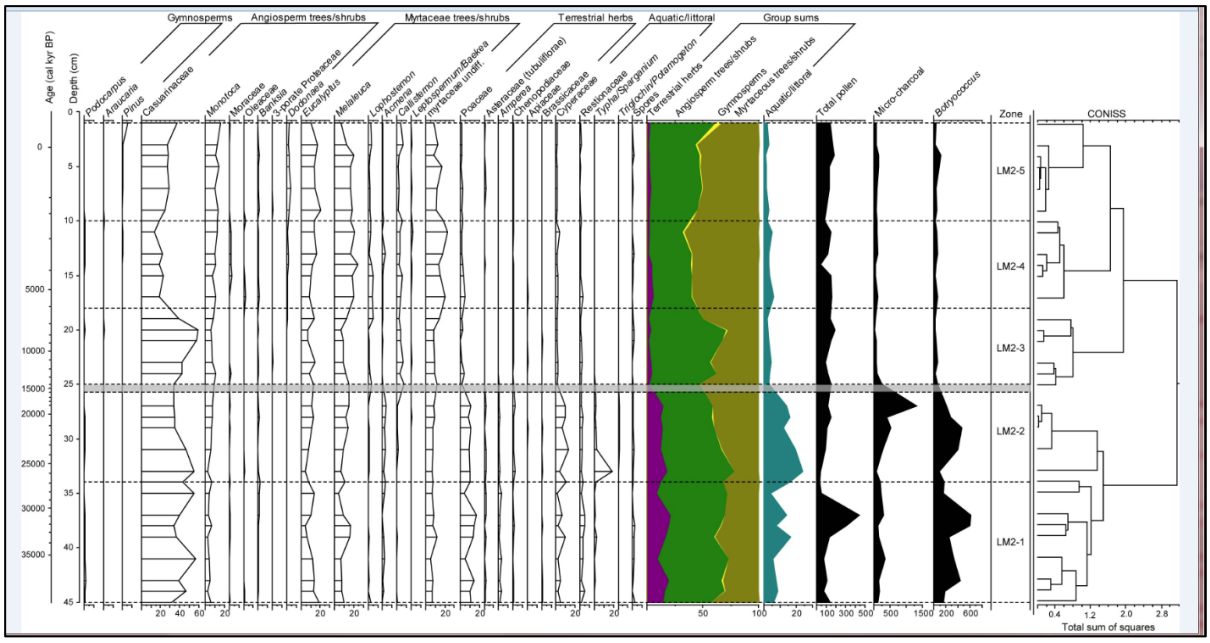
Gymnosperms
Angiosperm trees/shrubs
Myrtaceae trees/shrubs
Terrestrial herbs
Aquatic/littoral
Group sums
Age (cal kyr BP)
Depth (cm)
Podocarpus
Araucaria
Pinus
Casuarinaceae
Monotoca
Myrtaceae
Olearia
Banksia
S-hyrtle Proteaceae
Dodonaea
Eucalyptus
Melaleuca
Lophostemon
Kunzea
Callistemon
Leptospermum/Baeckea
Myrtaceae undiff.
Poaceae
Asteraceae (tubuliflorae)
Amaranthaceae/Chenopodiaceae
Apiaceae
Brassicaceae
Cyperaceae
Restionaceae
Typha/Sparganium
Trigrochin/Potamogeton
Sphagnum
Terrestrial herbs
Angiosperm trees/shrubs
Gymnosperms
Myrtaceous trees/shrubs
Aquatic/littoral
Total pollen
Micro-charcoal
Botryococcus
Zone
CONISS
LM2-5
LM2-4
LM2-3
LM2-2
LM2-1
Total sum of squares

Figure 5